Geomorphology 273 (2016) 361–373

Contents lists available at ScienceDirect

Geomorphology

journal homepage: www.elsevier.com/locate/geomorph

Spatial patterns of landslide dimension: A tool for magnitude mapping

Filippo Catani *, Veronica Tofani, Daniela Lagomarsino

Department of Earth Sciences, University of Firenze, Via La Pira, 4, Florence 50121, Italy

ARTICLE INFO

Article history:
Received 9 February 2016
Received in revised form 22 August 2016
Accepted 26 August 2016
Available online 27 August 2016

Keywords:
Landslide magnitude
Arno river basin
Intensity assessment
Spatial statistics

ABSTRACT

The magnitude of mass movements, which may be expressed by their dimension in terms of area or volume, is an important component of intensity together with velocity. In the case of slow-moving deep-seated landslides, the expected magnitude is the prevalent parameter for defining intensity when assessed as a spatially distributed variable in a given area. In particular, the frequency–volume statistics of past landslides may be used to understand and predict the magnitude of new landslides and reactivations. In this paper we study the spatial properties of volume frequency distributions in the Arno river basin (Central Italy, about 9100 km^2). The overall landslide inventory taken into account (around 27,500 events) shows a power-law scaling of volumes for values greater than a cutoff value of about 2×10^4 m^3. We explore the variability of the power-law exponent in the geographic space by setting up local subsets of the inventory based on neighbourhoods with radii between 5 and 50 km. We found that the power-law exponent α varies according to geographic position and that the exponent itself can be treated as a random space variable with autocorrelation properties both at local and regional scale. We use this finding to devise a simple method to map the magnitude frequency distribution in space and to create maps of exceeding probability of landslide volume for risk analysis. We also study the causes of spatial variation of α by analysing the dependence of power-law properties on geological and geomorphological factors, and we find that structural settings and valley density exert a strong influence on mass movement dimensions.

1. Introduction

A number of natural hazards are known to occur as stochastic processes whose magnitude frequency follows a non-normal distribution. Often, such a distribution assumes a form compatible with a power-law, an exponential or an extreme-value distribution. Widely known examples are e.g. the distribution of earthquakes, snow avalanches, landslides, volcanic explosions, epidemic spreading, meteorite impacts, forest fires and floods (Malamud and Turcotte, 1999; Malamud and Turcotte, 2006; Turcotte and Malamud, 2004; Clauset and Shalizi, 2009). The exponential decrease of frequency with increasing magnitude seems to be connected to patterns of self-organized criticality in complex systems as well as to the tendency towards optimal energy expenditure configurations (Bak et al., 1988; Rodriguez-Iturbe and Rinaldo, 1997), ubiquitous in natural systems. Sediment transfer pulses, including mass movements, do not seem to deviate from such a behaviour, even though the power-law form of magnitude–frequency distribution (MFD) is regarded as being mainly applicable to medium and large size occurrences.

Several studies address the statistical properties of MFDs making use of specific databases of landslides collected in several parts of the world (Guzzetti et al., 2002; van den Eeckhaut et al., 2007; Guzzetti et al., 2009; Trigila et al., 2010). In most cases such datasets constitute the sum of occurrences over large time spans and are thus called "historical inventories". In other cases, conversely, the properties of landslide ensembles triggered by a unique meteorological or seismic event are studied (Larsen and Torres-Sanchez, 1998; Dai and Lee, 2001). In the majority of the published material, the authors find a portion of the area (or volume) distribution (usually the higher tail) to follow a single or double power-law, expressed, according to the different cases, as a Gamma, Double Gamma, 3-parameters Gamma, Pareto, Generalized Pareto or Double Pareto distribution with a lower cutoff M_{min}. According to some views (see e.g. Stark and Hovius, 2001; Guthrie and Evans, 2004) the left part of the MFD (i.e. magnitude $m < M_{min}$) may be modelled as a positive-exponent power-low, but suffers from deviations and noise due to possible undersampling effects (Guzzetti et al., 2002; Malamud et al., 2004). Small occurrences are easily missed by field surveys or rendered invisible by vegetation regrowth, human activities and weathering processes on hillslopes (Guzzetti et al. 2002). This is especially true in historical inventories, where mass movements of different age are mapped together thus producing a statistical oversampling of the medium-large size events compared to smaller ones (Malamud et al., 2004).

Malamud et al. (2004) and Guzzetti et al. (2002) hypothesized that the left part of the distribution can be modelled by a different form of the same relationship, such as e.g. a power-law with different parameters and, possibly, a positive exponent. This inverse trend would be

* Corresponding author.
E-mail address: filippo.catani@unifi.it (F. Catani).

http://dx.doi.org/10.1016/j.geomorph.2016.08.032

explained by the prevalence of cohesive over frictional forces in the soil at small scales (Malamud et al., 2004; Van den Eeckhaut et al., 2007; Stark and Guzzetti, 2009). In such a case, the authors model the MFD of mass movements by supposing the presence of a double power-law distribution with different parameters (both with negative α_1 and α_2 exponents) across a characteristic cutoff scale M_{min} whilst, for dimensions smaller than a second cutoff M^*_{min}, by using a positive power-law ($\beta > 0$), in which the increasing influence of cohesion forces for smaller scales limits the number of mass movements that can develop.

The ubiquitous tendency of landslide hazard to occur according to this power-law scaling offers important insights on the underlying mechanisms for mass movement triggering and evolution, making it possible to predict the overall impact of climate changes in the near future trends for landslide-related risks (Convertino et al., 2013). Another important aspect of using known MFDs for mass movements is that they may be used as a robust basis for the forecasting of the magnitude (and thus of the intensity as defined by Fell et al., 2008 and Hungr, 1997), a fundamental step in natural hazard and risk prediction. In fact, for large areas, where slope-scale single-landslide intensity estimation is not possible, a statistical approach may often be the best solution, based on the MFD of area or volume. However, to be able to actually implement this approach, more quantitative information on the spatial variability of the MFDs of landslides in the geographical space is needed, a topic almost totally lacking in the relevant literature. In fact, in almost all cases (see e.g. Van den Eeckhaut et al., 2007 for a comprehensive listing) an entire landslide inventory is taken as a whole to produce a single MFD to be modelled by a given power-law scaling. This has been done for study areas ranging from 10^1 to 10^4 km^2 where very different geophysical and environmental conditions leading to sediment loss may coexist. Therefore, some important questions are still unanswered so far, such as: how well do such general MFDs depict local patterns of landslide magnitude? What happens to a scaling relationship when progressively moving from an area to an adjacent one with different geophysical settings? Can the power-law exponents be treated as random space variables with autocorrelation properties? In this paper we attempt to give a contribution in this direction. In particular, we study the spatial characteristics of the power-law scaling in a large and well-studied landslide volume frequency distribution (Arno river basin, central Italy, counting >27,000 events over about 9100 km^2) by computing a spatially variable set of MFD parameters as random space variables. We determine the spatial autocorrelation properties of such variables and propose a new simple tool to map the magnitude exceeding probabilities as a proxy for landslide intensity or potential destructive power. Then, we analyse the relationships between MFD parameters and environmental settings to explore the possible causes of this spatial variability.

2. Materials and methods

2.1. Working hypothesis

The starting hypothesis at the basis of this work is that the MFD of area and volume of mapped landslides in a given region shows a power-law scaling, at least for medium and large sized occurrences, and it is not spatially constant but varies continuously in space. As a corollary, the overall MFD computed over the entire inventory is an average quantity, which is locally stationary only for very homogeneous environmental conditions. We will, henceforth, refer to such environmental conditions as Landslide Conditioning Variables (LCVs), which may include geology, geomorphology, local climate, vegetation, land use, geomorphometry and hydrology. The hypothesis is supported by numerous studies as summarised by Van den Eeckhaut et al. (2007) for all types of landslide collections, either event-related or historical, made up by single or mixed typologies (such as e.g. shallow or deep seated slides, falls, and debris flows), related to large or small areas. We will also test this hypothesis experimentally over the test area. The characteristics of the inventory in the study area (Catani et al., 2005) are well suited to this approach because the majority of mapped landslides has slow rates of movement according to Fell et al. (2008) (rotational earth slides and solifluctions) which implies that their kinetic energy is essentially linked to dimensions, hence volume. In particular, earth slides constitute 77.4% of the total number and, furthermore, they consistently show higher-than-average volumes (Table 1) so that the right side of the empirical MFD is almost only occupied by a single typology.

A derivation of the main hypothesis is that a suitable subsetting of the entire inventory would produce sub-inventories equally representative in statistical terms that can be separately studied to understand possible linkages to the local characteristics of the sub-area. Therefore, the power-law fitting of the subsets would present MFD parameters locally valid that could then be compared to each other and, upon verification of continuity, treated as random space functions with definite autocorrelation properties. The second hypothesis is that, once the first one is verified and the local MFD parameters for the distribution chosen are autocorrelated in space, we can use geostatistical tools to study, interpolate and map the scaling properties of landslides thus producing magnitude estimation maps. In the study area, Catani et al. (2005) and Convertino et al. (2013) have previously computed area frequency statistics for the landslide inventory described in the area section. The authors found that a power-law scaling is a valid model for explaining the frequency distribution of mapped landslide areas for values greater than a cutoff of about 10^4 m^2 (1 ha). In particular, they adopted a power-law type distribution in the continuous form:

$$p(a)da = \Pr(a \le A \le a + da) = Ca^{-\alpha}da \tag{1}$$

where a is the landslide area and C is a normalization constant. For very small values of a this probability density diverges so that there must be a limiting or cutoff value to the power-law behaviour that can be denoted by a_{min}. In landslide systems, for both areas and volumes, the exponent α is always greater than unity. In this case, for landslide volume, we can find that:

$$p(v) = \frac{\alpha - 1}{v_{min}} \left(\frac{v}{v_{min}} \right)^{-\alpha} \tag{2}$$

where v is volume and v_{min} is the lower cutoff volume for which the power-law scaling holds. In the cumulative form:

$$P(v) = \int_v^\infty p(v\prime)dv\prime = \left(\frac{v}{v_{min}} \right)^{-\alpha+1} \tag{3}$$

In particular, if we limit the population to the tail of the empirical distribution ($v \ge v_{min}$) it must be:

$$P(\ge v_{min}) = \int_{v_{min}}^\infty p(v)dv = 1 \tag{4}$$

So that the exceedance probability for a given volume V ($\ge v_{min}$) can be obtained by integration of the previous equation in a given interval

Table 1
Landslide typology in the Arno river basin according to the latest available inventory. Only the three typologies considered in the study are reported.

Landslide typology	Frequency (%)	Total area (m^2)	Average area (m^2)	Average volume (m^3)
Earthslides	77.4	5.9×10^8	2.9×10^4	1.7×10^5
Flows	4.7	0.2×10^8	1.5×10^4	1.5×10^4
Solifluctions	17.9	1.9×10^8	3.7×10^4	3.7×10^4

$V \to \infty$:

$$P(\geq v) = \frac{\alpha - 1}{v_{\min}^{(-\alpha+1)}} \int_{V}^{\infty} v^{-\alpha} dv = \left(\frac{v}{v_{\min}}\right)^{(-\alpha+1)} \quad (5)$$

Eq. (5) gives the probability of occurrence of a landslide with volume greater than a given value V and can be used for modelling probability distributions of landslide magnitude over a given reference study area relative to the inventory used to estimate the $P(v)$ scaling parameters. An approach based on this model may represent a powerful tool for the computation of direct and inverse problems for the assessment of landslide volume probability in operational, risk mitigation applications.

2.2. Study area description

The area selected is the Arno river basin, in Central Italy, an area where a large database of over 27,000 landslides has been mapped recently (Catani et al., 2005). The Arno River basin has an area of about 9100 km^2 and is located across the Northern Apennine chain. This orogen is a complex thrust-belt system made up by the juxtaposition of several tectonic units, built up during the Tertiary under a compressive regime that was followed by extensional tectonics from the Upper Tortonian. The extensional phase produced a sequence of horst-graben structures with an alignment NW–SE: the grabens have been filled with marine (to the West) and fluvio-lacustrine (to the East) sediments (Martini and Vai, 2001) deposited from the Upper Tortonian to Quaternary. From a geomorphological point of view the Arno river basin is mainly hilly, with plains in which cohesive and granular fluvio-lacustrine sediments outcrop, and four mountain chains, mainly made of flysch rocks: Monti Pisani-Montagnola Senese, Monte Albano-Chianti, Calvana-Monte Morello-Pratomagno, and Monte Falterona-Mandrioli-Alpe di Catenaia (Fig. 1).

The study area is characterized by a temperate climate with a dry summer. These geological and climatic settings clearly affect the occurrence, typology and intensity of surface processes, primarily through differences in mechanical properties linked to prevalent lithologies. On this basis three main lithotechnical categories can be identified in the basin, such as cohesive and granular soils, hard rocks and soft rocks. The general annual rainfall pattern shows a minimum in July and two maxima: one in November and the other at the end of the winter. Mean values of yearly rainfall vary in relation to relief and location, ranging from 800 mm in the Chiana valley to 1800 mm on the Apennine ridges.

The landslide inventory of the Arno river basin, surveyed between 2003 and 2005 by a team of experienced field geomorphologists, counts >27,500 mass movements (Catani et al., 2005). This database was built as a starting point for landslide hazard and risk analysis and reports, for each landslide, information regarding the typology, the state of activity, the perimeter and the area. Detachment and deposition zones were mapped together. The inventory was organized following the approach proposed by Soeters and van Westen (1996) which consists of i) acquisition of literature and ancillary data such as existent inventories, ii) mapping from aerial photographs, and iii) field surveys and validation that represented a key step especially for the assessment of state of activity and validation of mobilized volumes.

The ancillary data and existing inventories used during the work were gathered from local universities, research institutes, municipalities and river basin authorities. Some of them date back to 1995 and in total they cover the entire territory of the Arno river basin. The aerial photos used in the analysis cover a period ranging from 1993 to 2000 and have spatial scales from 1:13.000 to 1:33.000.

In the database used, major landslide types are earth slides (20,575, 77.4%) and solifluctions (4774, 17.9%), followed by flows (1245, 4.7%) (Table 1). Other minor types of movements, such as falls and topples, have not been considered in this study. Regarding the state of activity, 60% of the mass movements are in a dormant state, 38% in an active

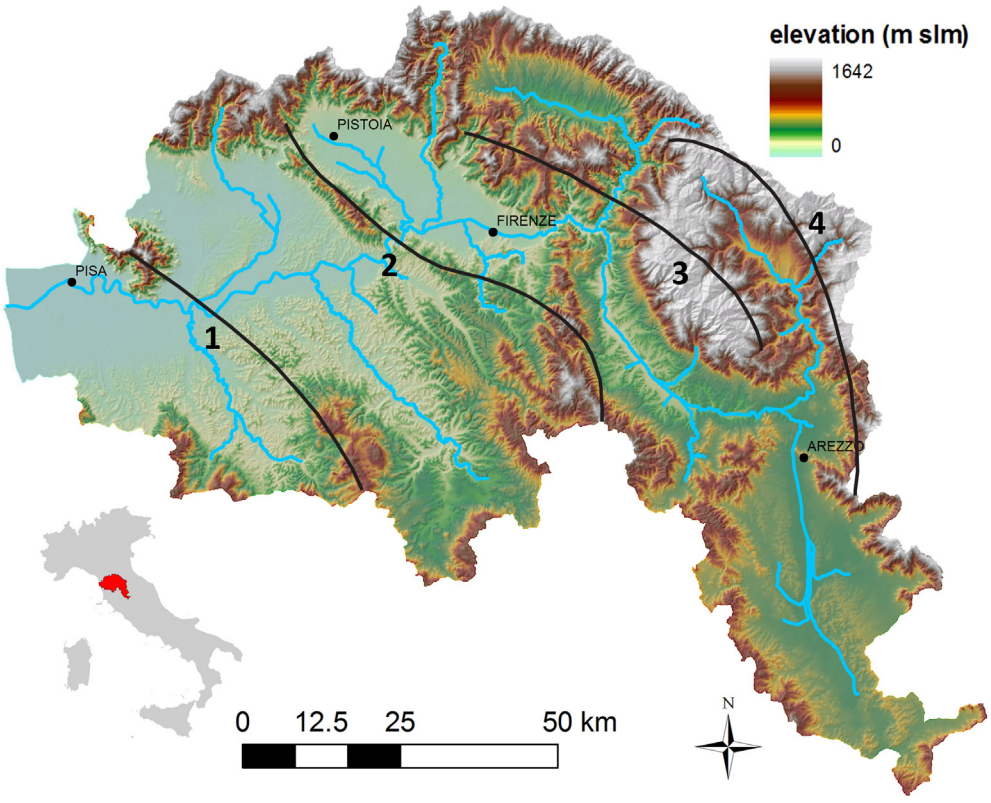

Fig. 1. Location and physiography of the Arno river basin. The main mountain ranges (according to Boccaletti et al., 1995) are highlighted with black lines: 1. Mt.Pisano-Montagnola Senese; 2. Mt.Albano-Monti del Chianti; 3. Calvana-Mt.Morello, Pratomagno; 4. Mt.Falterona-Mandrioli-Alpe of Catenaia.

state and only 2% are in an inactive or stabilized state. The landslide typologies largely depend on the morphological and geological settings of the Arno river basin. In general terms, in the eastern part of the basin corresponding to the Apennine chain, flysch formations and medium to high slope angles prevail, resulting in the dominance of earth slides. In the northern part of the basin, high slope angles and metamorphic

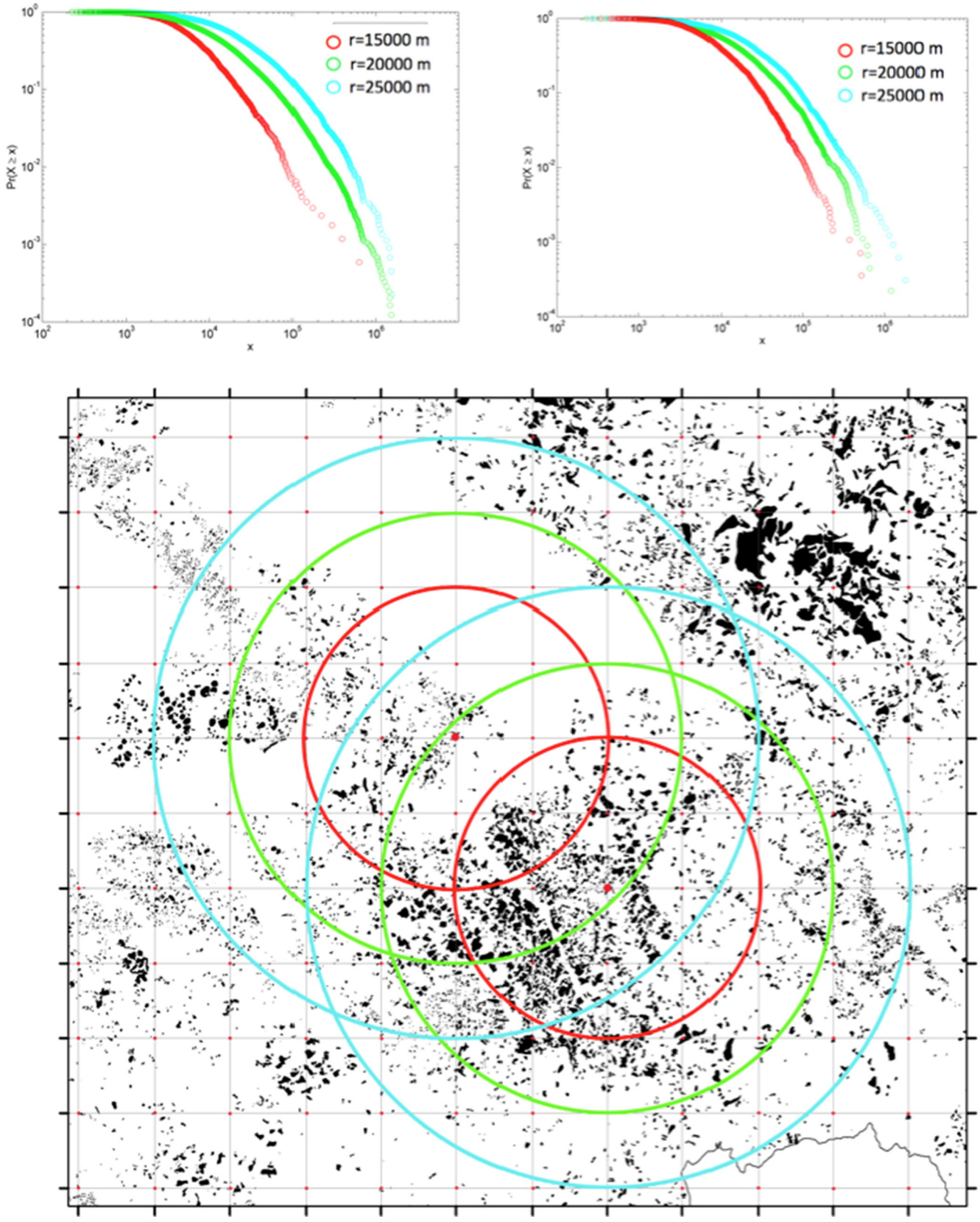

Fig. 2. Example of the definition of circular windows with different radius *r* relative to a portion of the study area. Inside each circle we define a subset of the landslide inventory by selecting those landslides whose barycentre falls within the circle itself and then we compute power-law statistics. The figure has only explanatory purposes and it is not to scale.

and hard rocks result in a prevalence of flow-type landslides, while in the central part characterized by low slope angles and cohesive and granular soils, shallow landslides such as solifluctions tend to prevail. Other types of landslides such as falls and topples are rare and mainly located in particular areas with specific geological conditions.

Landslide area ranges from 100 to 5×10^6 m^2. Most of the mass movements registered are rotational or planar slow-moving slides. A large number of them (about 90%) are characterized by recurrence, intermittency and velocities from extremely slow to very slow, according to the classification of Cruden and Varnes (1996) and Fell et al. (2008). For the majority of the mapped landslides we do not have information on the timing of the first activation.

To compute landslide volumes we have developed a simple procedure based on the assumption that slide intensity and kinetic energy are mainly connected to mass, since the movements are extremely slow to very slow. In particular, we have defined two different procedures; one for the rotational slides assuming a semi-ellipsoidal shape and the other for the remaining types of movement including shallow slides, solifluctions and flows, assuming a planar sliding surface with a constant depth. In the latter case we have computed the volumes assuming a constant average depth of 1 m, because Canuti et al. (2000); Bianchi and Catani (2002); Casagli et al. (2004); Catani et al. (2010) and Bicocchi et al. (2015, 2016) reported that an average soil thickness for shallow landslides in the Arno river basin was about 1.0 m with a standard deviation of 0.5 m. Concerning rotational slides, as already noted by Cruden and Varnes (1996), landslide mass and volume, can be computed by assuming a semi ellipsoidal shape. The volume is:

$$V = \frac{1}{6}\pi D_r W_r L_r \tag{6}$$

where D_r is the depth of the rupture surface, W_r is the width of the displaced mass and L_r is the length of the rupture surface. Starting from the inventory map in digital form, which represents landslide polygons in two dimensions over a projected geographic coordinate system, the average parameters of landslide geometry can be derived from the following assumptions: i) W_r and L_r are derived from the outline of the polygon, the slope angle and the distance between the scarp and the toe of the landslide through simple geometrical relations on a 10 m resolution digital terrain model (DTM); ii) D_r is computed following the relation proposed by Cruden and Varnes (1996) according to which the ratio of the D_r to L_r ranges between 0.15 and 0.33.

The application of such a computation to the inventory for the entire Arno river basin has shown that the volumes of the mapped landslides range between 10^2 and 10^7 m^3. The relationship between the area and volume of landslides is thus not linear, and the analysis of the distribution of volumes may provide a result different from that of the areas. In the case of intensity and energy estimation, volume is much more relevant than area; therefore, we focused on landslide volumes.

2.3. Methodology and experimental setup

We will limit our experimentation to the high-tail part of the MFD for which the power-law holds, without discussing whether or not there is another power-law relationship in the left part of the distribution. In any case, the methodology is repeatable for any power-law relationship which fits a portion of the MDF. To fit such a model to an empirical distribution, two parameters have to be determined: the scaling exponent α and the cutoff value v_{min}. The latter must be evaluated firstly, since the definition of α is linked to the normalization constant that gives $P(\geq v_{min}) = 1$.

There is no precise or repeatable way to estimate v_{min} even though in most cases an heuristic analysis of volume-frequency plots guided by the expert knowledge is used (Dai and Lee, 2001; Guzzetti et al., 2002; Brardinoni and Church, 2004; Van Den Eeckhaut et al., 2007). Our attempt, however, computes a large number of power-law fittings over the study area to explore the variations of volume scaling in space. In particular, we try to determine α and v_{min} at every arbitrary location in the study area using the method proposed by Clauset and Shalizi (2009), based on a suitable neighbourhood sampling of the inventory with a basic principle similar to that used by geographically weighted regression (Brunsdon et al., 1996). The neighbourhood can be of two types: spatially continuous (moving circular window covering a portion of the area) or thematic (sub-samples of the inventory based on environmental settings). According to Clauset and Shalizi (2009), the computation of α should be based on maximum likelihood estimation (MLE) since least-squares linear regression approaches may generate significant systematic errors for very small deviations in the tail of the distribution.

Landslide inventories are usually incomplete, due to the limitations of survey methods. Whilst such incompleteness in small-sized high-frequency occurrences does not produce relevant errors in the left part of the MFD, the opposite is true for the large-size low-frequency part of the MFD where even a single missed occurrence could produce a large error in the least-squares estimation of the power-law exponent. This problem can be avoided by using the MLE method according to which α can be estimated, for a sample fitting an exact power-law for $v > v_{min}$, as suggested by Clauset and Shalizi (2009):

$$\alpha = 1 + n\left[\sum_{i=1}^{n} \ln \frac{v_i}{v_{min}}\right]^{-1} \tag{7}$$

where n is the number of observed values for which $v \geq v_{min}$. The estimated value of α converges towards the true value in the limit of large n. The standard error thus depends strictly on n and is equivalent to:

$$\sigma = \frac{\alpha - 1}{\sqrt{n}} + O(1/n) \tag{8}$$

where $O(1/n)$ is a positive higher-order error. For estimating the value of α relative to a given sample or sub-sample of the population, the

Table 2
Identification code and physical characteristics of the selected UCUs. GCS: granular and cohesive soils; HR: hard rocks; SR: soft rocks. Only UCUs with Landslide # > 1000 have been considered in the discussion. For a more detailed discussion on how the various control variables are associated in the study area, please refer to Catani et al. (2013).

UCU	Profile curvature	Slope (°)	Lithology	Area (km^2)	Landslide #	Area landslide/area UCU
1.1.1	Concave	0–5	GCS	10.58	127	0.120
1.1.2	Concave	0–5	HR	9.61	18	0.010
1.1.3	Concave	0–5	SR	1.79	16	0.050
1.2.1	Concave	5–25	GCS	21.79	1694	0.880
1.2.2	Concave	5–25	HR	42.14	958	0.300
1.2.3	Concave	5–25	SR	4.34	608	0.170
1.3.1	Concave	>25	GCS	5.10	312	0.470
1.3.2	Concave	>25	HR	22.33	312	0.160
1.3.3	Concave	>25	SR	1.23	41	0.270
2.1.1	Planar	0–5	GCS	2612.85	208	0.002
2.1.2	Planar	0–5	HR	184.32	24	0.002
2.1.3	Planar	0–5	SR	103.47	19	0.092
2.2.1	Planar	5–25	GCS	1735.95	4486	0.070
2.2.2	Planar	5–25	HR	2312.46	4430	0.090
2.2.3	Planar	5–25	SR	911.63	3249	0.150
2.3.1	Planar	>25	GCS	103.19	360	0.020
2.3.2	Planar	>25	HR	750.36	857	0.030
2.3.3	Planar	>25	SR	50.65	76	0.020
3.1.1	Convex	0–5	GCS	11.29	189	0.190
3.1.2	Convex	0–5	HR	8.30	20	0.008
3.1.3	Convex	0–5	SR	2.44	27	0.060
3.2.1	Convex	5–25	GCS	39.85	2803	0.760
3.2.2	Convex	5–25	HR	85.05	1601	0.440
3.2.3	Convex	5–25	SR	13.73	1359	0.170
3.3.1	Convex	>25	GCS	10.53	170	0.210
3.3.2	Convex	>25	HR	55.31	374	0.100
3.3.3	Convex	>25	SR	3.74	47	0.100

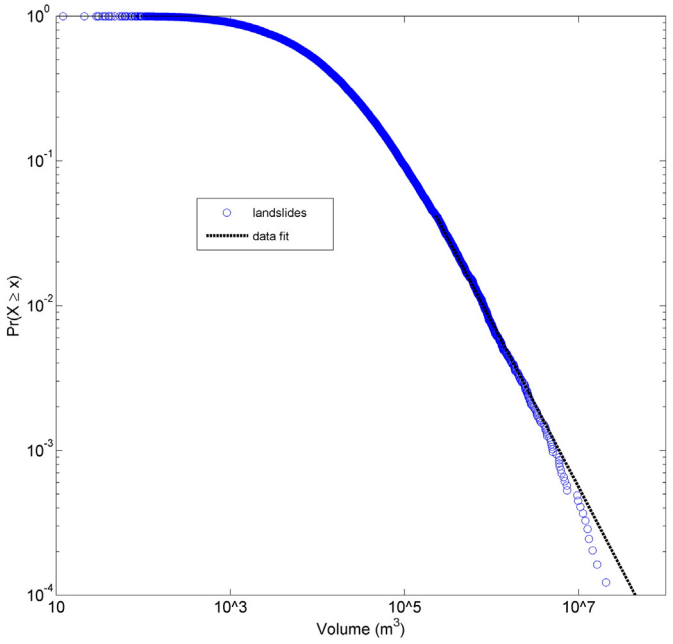

Fig. 3. Frequency-volume plot for the complete database of Arno river basin landslides.

value of v_{min} must be known in advance. In agreement with Clauset and Shalizi (2009) we estimate this cutoff value by using a Kolmogorov-Smirnov (KS) scheme which exploits the minimization of the difference between the observed and best-fit modelled power-law CDFs for increasing values of v_{min} until we find the best estimate. The KS statistic approach is considered a standard measure to quantify the distance between two probability distributions for non-normal data (Press et al., 1992).

The accuracy in the estimation of the power-law statistics is always proportional to the number of observations in the given sample. Whilst the error in the estimation of α is given by Eq. (8), the error in the assessment of the optimal v_{min} value by using KS statistics is difficult to measure but known to become insignificant for $n(v \geq v_{min}) > 1000$ (Clauset and Shalizi, 2009). Starting from this hypothesis and methodological basis, we use the data set presented in the previous section to perform the following tests.

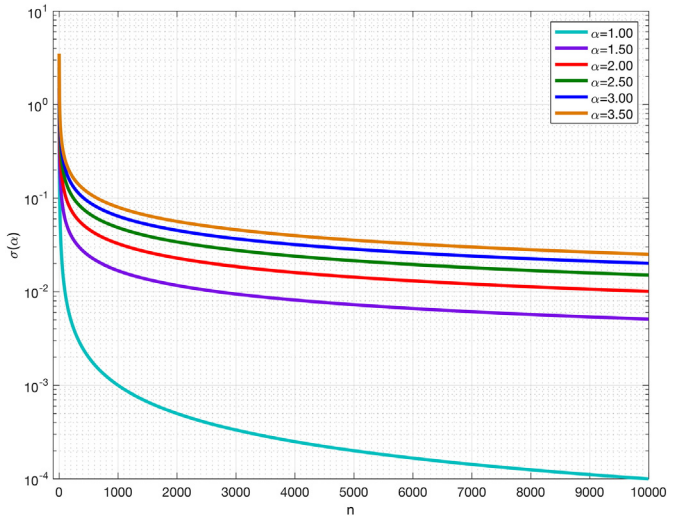

Fig. 4. Theoretical variation of the standard error σ as a function of n for different α values.

Firstly, we compute the overall power-law statistics of landslide volumes for the dataset as a whole. Then, we define lattices of M equally spaced points in the coordinate space of the study area, and for each point, we draw circular moving windows of radius r. Then, for each circular window, we define a subset of the landslide inventory by selecting those landslides whose barycentre falls within the circle itself. Therefore, we have at this stage M subsets, which may be mutually joint or disjoint, each one belonging to the relative circle with centre in C_i, for which we can compute power-law statistics as indicated. We thus end up with a lattice of M pairs of α and σ values for each point that we treat as random space variables. We test this for increasing values of the moving window radius r, from 5×10^3 to 5×10^4 m, a dimension almost encompassing the entire Arno river basin (Fig. 2).

For each r we generate a field of α and σ values of which we study the spatial distribution and autocorrelation properties. In particular, by analogy with other geophysical attributes of the landscape, it is possible to define a landslide MFD covariance function, which reflects the average degree of correlation in α between arbitrary points separated by a

Table 3
Max, min, mean, standard deviation of the number of landslides in circles (n), α and σ (standard error in the estimation of α according to Eq. (8)) with 95% confidence intervals (c.i.) for the estimation of mean(α) and mean(σ) at increasing circle radius r.

	Max	Min	Mean	Std dev	95% c.i. low	95% c.i. high
$r = 5$ km						
n	250	30	67	36	–	–
α	3.142	1.517	1.994	0.284	1.954	2.035
σ	0.419	0.059	0.152	0.062	0.143	0.161
$r = 10$ km						
n	686	30	155	114	–	–
α	3.526	1.531	2.038	0.282	2.010	2.066
σ	0.463	0.039	0.116	0.066	0.109	0.122
$r = 15$ km						
n	994	30	277	219	–	–
α	3.171	1.532	2.037	0.261	2.014	2.060
σ	0.370	0.027	0.092	0.061	0.087	0.098
$r = 20$ km						
n	1336	30	420	346	–	–
α	3.167	1.549	2.020	0.216	2.007	2.045
σ	0.341	0.020	0.070	0.053	0.074	0.083
$r = 25$ km						
n	1836	31	934	1276	–	–
α	3.001	1.549	2.020	0.216	2.004	2.037
σ	0.341	0.020	0.070	0.053	0.066	0.074
$r = 30$ km						
n	2575	30	1303	1800	–	–
α	2.683	1.539	2.000	0.187	1.987	2.014
σ	0.253	0.018	0.059	0.042	0.056	0.062
$r = 35$ km						
n	3118	30	1574	2184	–	–
α	2.458	1.547	1.990	0.169	1.978	2.002
σ	0.225	0.016	0.050	0.036	0.048	0.053
$r = 40$ km						
n	3550	35	1793	2485	–	–
α	2.477	1.569	1.984	0.156	1.974	1.995
σ	0.215	0.015	0.043	0.030	0.041	0.045
$r = 45$ km						
n	3986	30	2008	2797	–	–
α	2.497	1.563	1.979	0.144	1.969	1.989
σ	0.307	0.014	0.039	0.029	0.037	0.041
$r = 50$ km						
n	4247	36	2142	2987	–	–
α	2.253	1.593	1.972	0.129	1.963	1.981
σ	0.177	0.014	0.033	0.021	0.032	0.035

given distance λ. The covariance function is defined, for a given direction x, by:

$$C_\alpha(\lambda) \propto \langle \alpha(x)\alpha(x+\lambda)\rangle_x \quad (9)$$

In our assumption, $C_\alpha(\lambda)$ is a measure of the heterogeneity of the volume frequency size distribution for landslides with $v \geq v_{min}$. According to random function theory, by using this covariance it is possible to define two typical scales: microscales and macroscales (Bras and Rodriguez-Iturbe, 1985; Tucker et al., 2001) of the processes affecting landslide dimensions in a given area. The smaller scale λ^* represents the distance over which the power-law exponent α varies due to local factors, whilst the macroscale Λ defines the distance over which the tails of the probability density function (PDF) of landslide volumes becomes uncorrelated, which is equivalent to the classical autocorrelation distance in geostatistics under the assumptions of isotropy and second-order stationarity.

The estimation of Λ for a given area may give important information on the scale of aggregation of landslide clusters of the same typology and, possibly, the same triggering factors. The last stage of this experimentation concerns the construction of magnitude maps based on the spatial power-law statistics. In particular, we use the autocorrelation properties of the modelled MFDs to interpolate continuous fields of α and v_{min} to be used for producing maps of exceedance probability for given landslide volumes. Finally, to try to understand which are the causes of MFD variability in space, we define a different type of subset for testing the dependency of MFD on three landslide conditioning variables (LCVs): lithology, slope angle and landcover. We chose only three LCVs to limit spatial fragmentation and maintain the statistical significance of subsamples. Among all the possible LCVs already studied in the area by Catani et al. (2013), we selected the three because they were revealed as the most important factors affecting landslide area and volume (e.g. Frattini and Crosta, 2013).

In other words, we assume that meaningful power-law distributed subsets can be created in a spatially non-contiguous field, i.e. aggregating landslides in areas with similar LCV settings. Therefore, according to a classification scheme derived for the area (Catani et al., 2005, 2013), the three LCVs are combined by using GIS-based raster overlay to build a continuous Unique Condition Unit (UCU) coverage for the test site, as proposed originally by Carrara et al. (1991) and afterwards widely adopted in landslide susceptibility studies.

In particular, each LCV is divided in three classes so as to obtain 27 possible UCU combinations. The landslide inventory is then sampled by using the thematic UCU classes to produce an ensemble of 27 subsamples for which power-law statistics are computed following the approach proposed by Clauset and Shalizi (2009). Table 2 specifies the characteristics of each class for lithology, slope angle and landcover, and the area and the number of landslides for each UCU. The class limits have been chosen with two aims: i) to limit the number of total UCUs for avoiding unrepresentative samples of the population; and ii) to maximize the discriminant power of LCVs according to previous studies on landslide susceptibility in the Arno river basin (Catani et al., 2005, 2013).

3. Results

3.1. Global MFD

The inventory taken as a whole shows a power-law scaling of volumes for values greater than a cutoff v^*_{min} of about 2×10^4 m^3 (Fig. 3). For volumes $v \geq v^*_{min}$, the α^* and σ^* values computed using Eqs. (7) and (8) are $\alpha^* = 2{,}1453$ and $\sigma^* = 0{,}0355$, respectively. This value of α^* is higher than those reported by Brunetti et al. (2009), where 19 different landslide databases are analysed with α^* values ranging from 1 to 1.9. It must be considered, however, that we evaluate the distribution of 27,000 events, whereas the previous datasets include at most about 3000 landslides for each.

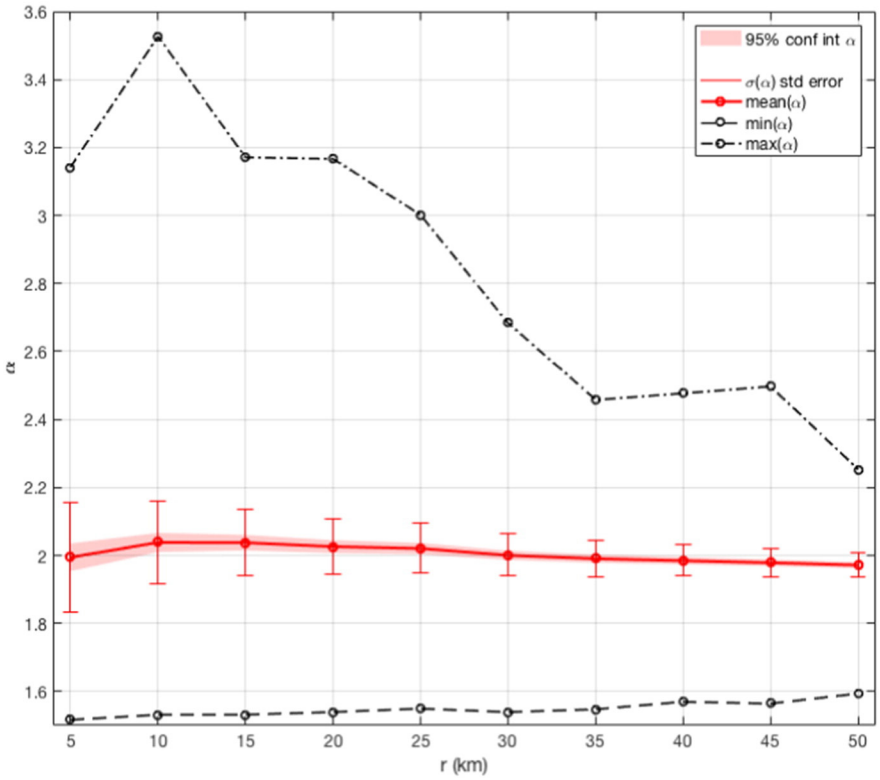

Fig. 5. Variation of α_{max}, α_{min} and $\bar{\alpha}$ as a function of circle radius r. Error bars on $\bar{\alpha}$ refer to corresponding computed standard errors σ. Shaded area around $\bar{\alpha}$ line shows 95% confidence intervals.

Table 4
Autocorrelation properties at varying radius r. The azimuth angles Θ and θ refer to the main axis of the anisotropy ellipse. Λ and λ are in km.

r(km)	Λ_{max}	Λ_{min}	$\Theta(^\circ)$	λ_{max}	λ_{min}	(θ°)
5	86.3	23.5	304	26.8	14.1	43
10	143.0	26.1	299	34.5	19.7	60
15	153.0	34.5	297	41.4	27.5	66
20	164.0	36.7	297	51.7	29.2	78
25	171.0	46.1	297	171.0	30.3	65
30	185.0	49.3	301	185.0	32.4	65
35	188.0	58.2	304	188.0	41.5	65
40	19.00	5.94	307	19.00	3.32	63
45	19.00	6.82	311	19.00	4.19	64
50	19.00	6.82	316	7.68	3.32	86

3.2. Moving window statistics

We selected a lattice of $M = 832$ points p_i covering the study area with a 5 km inter-distance. Each point p_i represents the centre of a search circle of variable radius r. For r values between 5 and 50 km with a 5 km step, we defined the M subsets of the landslide inventory included within the circles $S(p_i; r)$ and we computed the quantities $\alpha_{i,r}$ and $\sigma_{i,r}$. As we have seen, the accuracy σ in the maximum likelihood estimation of α strongly depends on the total number of landslides in the subsample. In theory, the expected standard error can be estimated by using Eq. (8) for a given α value. Fig. 4 depicts the variation of the standard error σ as a function of the number of elements n in the subsample for some typical values of the parameter α as found in the experimental fit of landslide inventories worldwide (Van den Eeckhaut et al., 2007). Any estimate of α is affected by error, which is unacceptably high for $n < 10^2$ (Fig. 4). We intend to compare α values for different locations (at r = constant) and to discriminate whether their differences are due to estimation errors or actual variations in the local factors. Since we have different values of n for each circle, the relative $\alpha_{i,r}$ will be always coupled with $\sigma_{i,r}$ so that only values of $\Delta\alpha = \alpha_{i,r} - \alpha_{i+1,r}$ greater than the expected standard error will be regarded as meaningful. As expected, the average number of landslides falling into the circles increases with increasing r from $\overline{n} = 66.7$ for $r = 5$ km to $\overline{n} = 2142$ for $r = 50$ km. So does the mean accuracy in the estimation of α as expressed by decreasing values of σ from $\overline{\sigma}(r = 5) = 0.152$ to $\overline{\sigma}(r = 50) = 0.033$. A synthesis of the main results is listed in Table 3 whilst the overall variation of experimental values with r is shown in Fig. 5 along with the corresponding maximum σ value for each radius.

There is a high range $R_\alpha = (\alpha_{max} - \alpha_{min})$ for $r < 35$ km, well over the expected errors. This changes for $r > 35$ km, where R_α becomes almost comparable to the corresponding σ value, indicating that the variations of landslide volume are masked by data aggregation that compensates for local differences. The plot of Fig. 5 only reports extreme values and the average of α so it is not possible to appreciate the point-wise variations of the power-law parameter.

A more in-depth analysis is offered by looking at $\Delta\alpha$ as a function of r and geographic position by using $C_\alpha(\lambda)$ and estimating Λ. We computed the autocorrelation distances through correlogram analysis with anisotropy for each search radius over the entire study area, both with and without trend removal. Covariance properties relative to non-detrended fields should convey information on the macroscale characteristics of landslide volumes, whilst residual covariance after detrending should depict the autocorrelation properties due to local conditioning factors. In particular, the average range (i.e. the autocorrelation distance) at the macroscale will be regarded as a measure of Λ. The results are listed in Table 4; for each r, we report the minor and

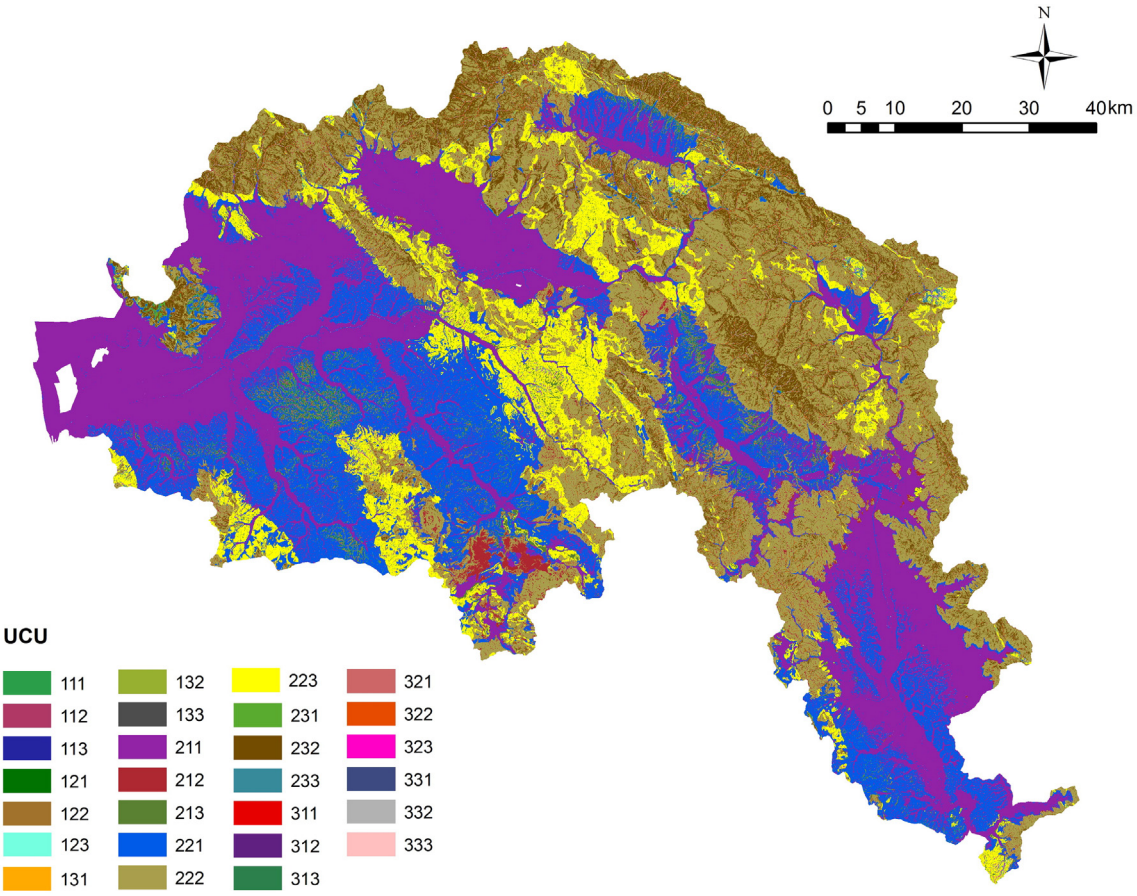

Fig. 6. Distribution of the Unique Conditions Units in the Arno river basin. For the definition of UCU numerical codes please refer to Table 1.

Table 5
UCU fit power-law parameters for the seven highly significant UCUs (see text for details).

UCU	α	V_{min} (m^3)	σ
1.2.1	2.2696	1.92×10^4	7.44×10^{-2}
2.2.1	2.0615	5.02×10^4	3.66×10^{-2}
2.2.2	2.2009	5.76×10^5	8.85×10^{-2}
2.2.3	2.0562	1.38×10^5	5.40×10^{-2}
3.2.1	2.3137	4.70×10^4	7.34×10^{-2}
3.2.2	2.1253	3.81×10^4	6.23×10^{-2}
3.2.3	2.3267	5.76×10^4	1.07×10^{-1}

major ranges (Λ_{min} and Λ_{max}), their detrended counterparts (λ^*_{min} and λ^*_{max}) and the azimuth angles of the main axis of the anisotropy ellipses (Θ and θ). The global covariance dimension, in terms of non-detrended autocorrelation distances (in km) increases with increasing radius, as expected due to data aggregation and overlapping, from $\Lambda_{max} = 86.3$ km at $r = 5$ km to $\Lambda_{max} = 190$ km at $r = 50$ km. Lower autocorrelation is conversely shown by the detrended α-field, where $\lambda^*_{max} = 26.8$ km at $r = 5$ km and $\lambda^*_{max} = 34.5$ km at $r = 10$ km. This is also expected due to the greater relative weight of local factors after detrending. As soon as the radius of search circles is increased, however, the local effects become again masked out by data aggregation until, at $r \geq 25$ km, λ^*_{max} tends to be close to Λ_{max}. Interestingly, anisotropy is much more evident in global (non-detrended) data (covariance ellipse flattening $\Lambda_{min}/\Lambda_{max}$ is always < 0.36) with an orientation of the main axis of the corresponding ellipse along a WNW–ESE direction ($\langle\Theta\rangle \sim 300°$), compatible with the general direction of the Apennine chain. The detrended counterparts show a much lower degree of asymmetry for radii $r \leq 20$ km, with reduced ellipse flattening $\lambda^*_{min}/\lambda^*_{max} > 0.5$, and conversely, marked asymmetry for larger radii ($\lambda^*_{min}/\lambda^*_{max} > 0.23$). Remarkably, the average direction of this asymmetry is very different from the global one described above, with $\langle\theta\rangle \sim 60°$, thus roughly oriented along the WSW–ENE direction which is transverse to the main mountain chains in the area.

3.3. UCU-based statistics

Fig. 6 shows the spatial distribution of the 27 UCUs in the Arno River Basin. It can be observed that the most common UCUs are 2.1.1 (areas with planar curvature, slope angles of 0–5°, and granular and cohesive soils), 2.2.2 (areas with planar curvature, slope angles of 5–25° and hard rocks) and 2.2.1 (areas with planar curvature, slope angles of 5–25°, and granular and cohesive soils). The former UCU corresponds to the fluvio-lacustrine plains while the latter corresponds to part of the mountain chains of the Arno River Basin (Fig. 1). The highest number of landslides occur in UCUs 2.2.1, 2.2.2 and 2.2.3 which are areas with planar curvature, slope angle between 5° and 25°, and cohesive and granular soils, hard rocks and soft rocks respectively (Table 1). A still high number of landslides can be found in UCU 3.2.1 with convex curvature, slope angles of 5–25°, and cohesive-granular soils.

Results on the spatial distribution of α show that local and global LCVs may affect volume frequency distribution. To inspect this possible dependency, we have obtained MFD plots differentiated on the basis of LCV combinations that do not give direct information on the spatial arrangement of landslide volume but can reveal important insights into the role played by environmental settings in shaping the magnitude distribution of slope processes. To compute MFD parameters, we have selected only the UCU with >1000 landslides. This value has been defined according to Clauset and Shalizi (2009) since distributions with >1000 samples provide MFD values with a higher significance and a lower computational error. Given that, values of α, v_{min} and σ have been computed for the seven UCUs (Table 5). The values of α show a low variance, ranging from 2.06 for UCU 2.2.3 to 2.33 for UCU 3.2.3. On the contrary v_{min} values are much more variable ranging from 1.92×10^4 m^3 for UCU 1.2.1 to 5.76×10^5 m^3 for UCU 2.2.2. Fig. 7 shows the MFD plots for the seven UCUs.

4. Discussion

The α field obtained by the procedure depicted in Section 3.2 seems to be well autocorrelated over a wide range of scales of aggregation and at two distinct scales of physical processes, as described by the Λ and λ^* statistics. The local and global maximum autocorrelation distances λ^*_{max} and Λ_{max} tend to become equal for scales of aggregation >25 km, suggesting that this is probably a threshold distance for data aggregation in order that local trends in the landslide volume scaling remain visible and significant in the study area. For larger scales of aggregation, the autocorrelation mainly depends on the overall probability distribution of landslide volumes, and local details are lost.

However, the autocorrelation also depends on orientation. The anisotropy in local weakly-aggregated data is not very evident and has an orientation of WSW–ENE almost perpendicular to the main axis of the Neogenic extensional basins, suggesting that local trends of landslide size may be partially dictated by the settings of hillslope materials along these geological structures. A much higher asymmetry is evident in regional, strongly aggregated data with the main axis direction of WNW–ESE, parallel to the main trend of the Apennine chain and to

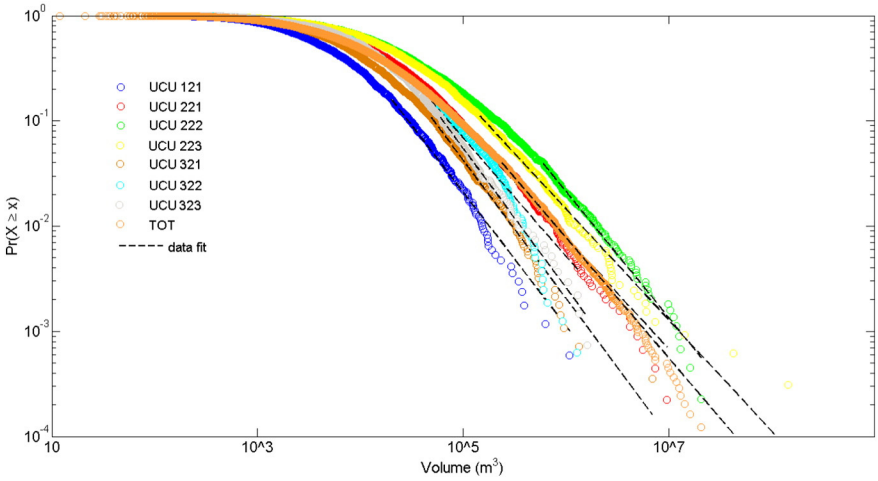

Fig. 7. CDF plots relative to the most representative UCUs compared to the one relative to the whole inventory (TOT). Dashed lines represent power law fits. Only UCUs with Landslide # > 1000 have been considered in the discussion of results.

the axis of sedimentary successions from the Oligocene flysch units (east side) to the Fold-and-Thrust belt (west side).

By using autocorrelation results to define the surface distribution of α values over the theoretical distances for local and global trends in landslide size distribution, we come up with maps depicting the MFD of landslides quantitatively at various scales. In particular, assuming a distance threshold $R_{th} = 25$ km, we aggregated landslide volume data with the moving window radius $R_\lambda = 15$ km for the local autocorrelation distance and $R_\Lambda = 35$ km for the global distance. Therefore, we adopted autocorrelation distances relative to the anisotropy ellipse of $\lambda_{max} = 41.5$ km, $\lambda_{min} = 27.5$ km, and $\Lambda_{max} = 188$ km and $\Lambda_{min} = 58.2$ km to perform Kriging interpolation to obtain continuous fields of α and σ.

The resulting continuous surfaces with a pixel size of = 500 m provide a spatially averaged estimation of the α and σ fields to be used in the forecasting of expected landslide volumes at any given point. The maps are represented in Figs. 8 and 9 and depict the variation of the power-law statistics over the study area using a colour ramp for α overlain by contour lines of σ at two scales R_λ and R_Λ. In both maps a greater importance of relatively larger landslide dimensions (lower power-exponents, red colours) in the north-eastern part of the Arno river basin is apparent. At the local scale image (Fig. 8), however, we find some smaller areas with low α values to the south-west, where the catchment boundary touches the fringes of low-relief hill areas of the Montagnola Senese range, and to the north, where the Montagna Pistoiese area shows distinctive MFD characteristics with respect to the areas to the east. Such differences are not visible when we remove local trends and we only look at larger scales (Fig. 9).

A better insight into the possible causes of the spatial variation of MFD in the study area comes from the results of the UCU analysis (Fig. 7). Here, UCUs 1.2.1, 3.2.1, 3.2.2 and 3.2.3 show volumes lower than the average of the total inventory. Such UCUs correspond to areas with convex curvature, medium slope angles (5–25°), and any lithology, or to areas with concave curvature, medium slope angles, and cohesive and granular soils. Instead, UCUs with landslide volumes higher than the average belong to the classes 2.2.2 and 2.2.3 that correspond to areas with planar curvature, medium slope angle, and soft or hard rocks. What makes the UCU volumes so different is not the variation of the power-law exponent (corresponding to α) that is very similar for all the UCUs, but the variability of v_{min} (or rollover). This suggests that hillslopes with marked curvature (both concave and convex) at the scale of analysis generally exhibit lower v_{min} than planar slopes. In other words, curved slopes show an MFD rollover at smaller volumes and the power-law has a larger range of validity than in planar slopes. A possible explanation of this behaviour is that there is a general correlation between landslide dimension and average valley width in a given area that, in turn, is reflected in the spatial distribution of minimum and maximum sizes of the mass movements that can take place within the valley limits. This is a finding which is not new (e.g. Fan et al., 2012; Roering et al., 2015) but which is of key importance in driving the spatial distribution of volumes.

In the study area, the average valley width in the hilly and mountainous regions, which is related to drainage density, seems to show increasing values from south to north, but there is obviously no clear trend due to the inherent hierarchical and fractal structure of river basins (Rodriguez-Iturbe and Rinaldo, 1997). An example of analysis of the spatial distribution of valley density and valley width in the Apennines is provided by Tucker et al. (2001) for an area adjacent to the Arno river basin. They show the existence of two autocorrelation dimensions for local and regional scales which are linked, respectively, to the catchment area and to the Apennines range orientation. If the same behaviour may be hypothesized for the Arno basin, on the southern side of the Apennine chain with respect to the area studied by Tucker et al. (2001), then the spatial distribution of maximum landslide size would be following an inverse topographic trend: increasing downvalley locally, but increasing from south to north regionally. This

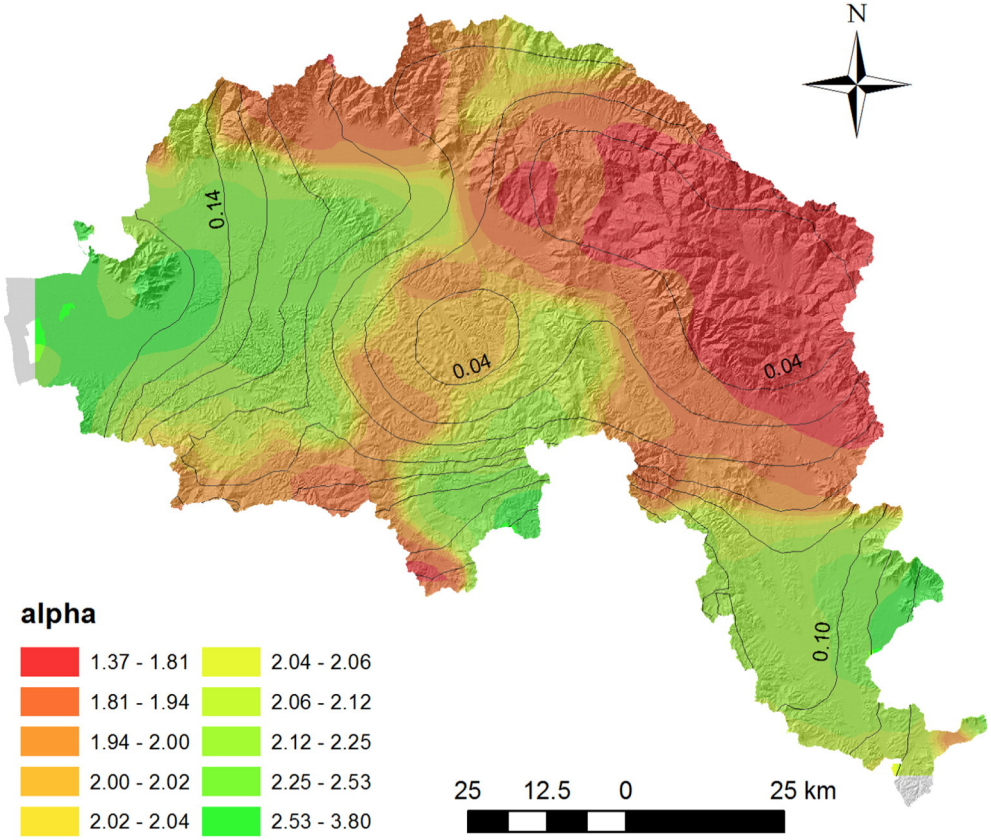

Fig. 8. Map of local α field obtained by using aggregation level r = 15 km. Contour lines represent isovalues of standard errors σ computed according to Eq. (8). (see text for details).

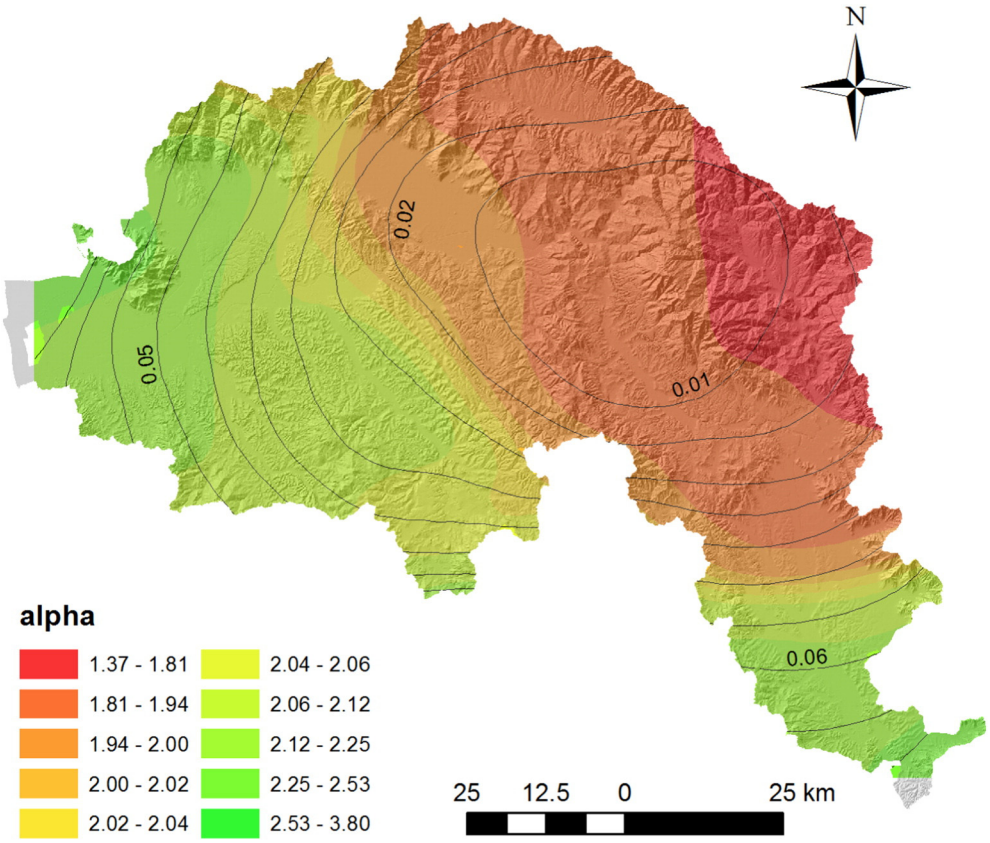

Fig. 9. Map of global α field obtained by using aggregation level $r = 35$ km. Contour lines represent isovalues of standard errors σ computed according to Eq. (8) (see text for details).

hypothesis seems to be supported also by a recent study by Tacconi-Stefanelli et al. (2016) which explores the comparison between valley width and landslide volume as a limit for landslide damming in Italy.

The UCU analysis reveals also a possible role of lithology in volume distribution as defined by α and v_{min} and shown by the maps in Fig. 10. Larger landslide dimensions (high v_{min} and lower power-exponents; red colours in Fig. 10) can be observed in the various mountain ranges of the Arno River Basin. Lower dimensions (low v_{min} and high power-exponents) are distributed in the SE and SW portions of the basin, displayed in yellow-green colours. Intermediate values of volume dimensions are observed in the central part of the basin (orange colour).

In general, the volume distributions within UCUs are in agreement with those derived from the moving window statistics (Figs. 8 and 9). In particular, larger landslide volumes are distributed along the main reliefs in the NE portion of the basin, while moving to the SW, where cohesive and granular soils outcrop, landslide dimensions generally decrease. In particular, v_{min} decreases from NE to SW and the power-law holds for a wider range of landslide dimensions. Thus, areas where cohesive and granular soils dominate have consistently lower volumes than areas where flysch and other stratified and massive rocks are prevalent. This result is in accordance with the findings of Frattini and Crosta (2013) and suggests the existence of a set of domains and scales where cohesive forces overcome frictional ones in surface deposits and regolith cover, as proposed by Stark and Guzzetti (2009).

Tectonic forcing could also be a driver of landslide size in the Arno river basin. Here, Balestrieri et al. (2003) and Cyr and Granger (2008) measured recent and present-day uplift rates ranging from 0.2 ± 0.1 to 1.0 ± 0.1 mm yr^{-1} moving from SW to NE. D'Anastasio et al. (2006), however, found a general lack of evidence of net elevation changes in the last 150 years by means of geodetic levelling, thus supporting the hypothesis of an uplift compensated by erosion. The Arno river basin, therefore, seems to be in a steady state at present, in which erosion rates balance rock uplift. Recently Roering et al. (2015) hypothesize that, in steady state conditions, greater uplift rates lead to larger and more frequent landslides. This hypothesis may well hold for the study area, and could help explain the general increase of landslide magnitude from SW to NE shown in Fig. 9. This would suggest a linkage between uplift rates and landslide volumes.

The importance of modelling and mapping the landslide volume distribution over large areas cannot be underestimated in risk analysis, because it provides users with a simple and effective tool to spatially estimate magnitude, which is a fundamental step for defining landslide intensity. We have seen that knowledge of the α field is a key for predicting the exceedance probability of a landslide occurrence with a given volume around a given point, according to Eq. (5). If we choose a reference volume of 10^5 m^3, which is a typical landslide volume capable of producing significant damage but still quite common in the study area, we can depict the exceedance probability of a given occurrence overcoming the threshold as in Fig. 11. This kind of map can be of direct use in landslide risk management at different working scales for defining intensity scenarios as suggested by the standard methodologies (see Corominas et al., 2013 for a recent review). Similarly, it is also possible to map the expected landslide volume $v(P_{exc})$ which is exceeded at a constant probability P_{exc} using the equation:

$$v(P_{exc}) = v_{min} P_{exc}^{\frac{-1}{\alpha - 1}} \quad (10)$$

Using a map like Fig. 11, we can show the probability of having a landslide with a certain volume such as $v > 10^5$ m^3 for each location. Provided that the standard error σ is small enough at each location, the exceeding probability or the volume exceeded can be determined using either the local (λ^*) or global (Λ) autocorrelation distances according to the scale of the study.

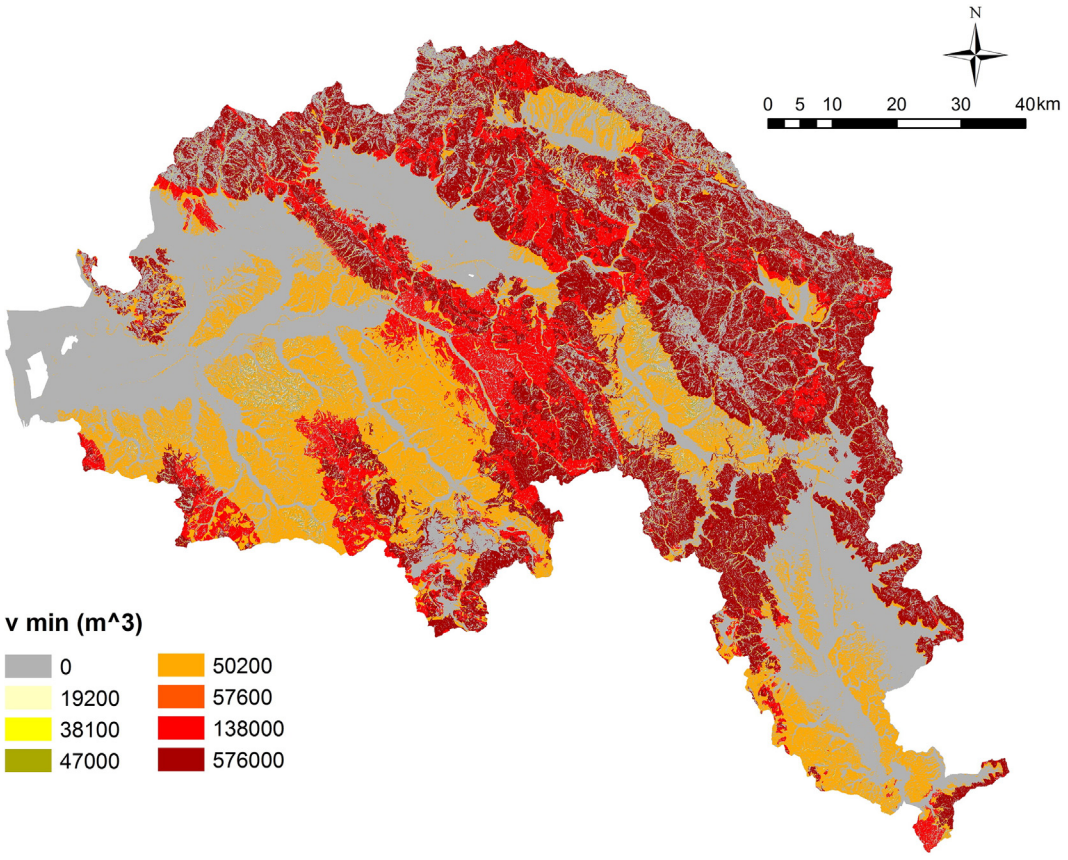

Fig. 10. Spatial distribution of v_{min} values over the UCUs in the study area. The lower the v_{min} the larger the range of landslide volumes represented in the power-law.

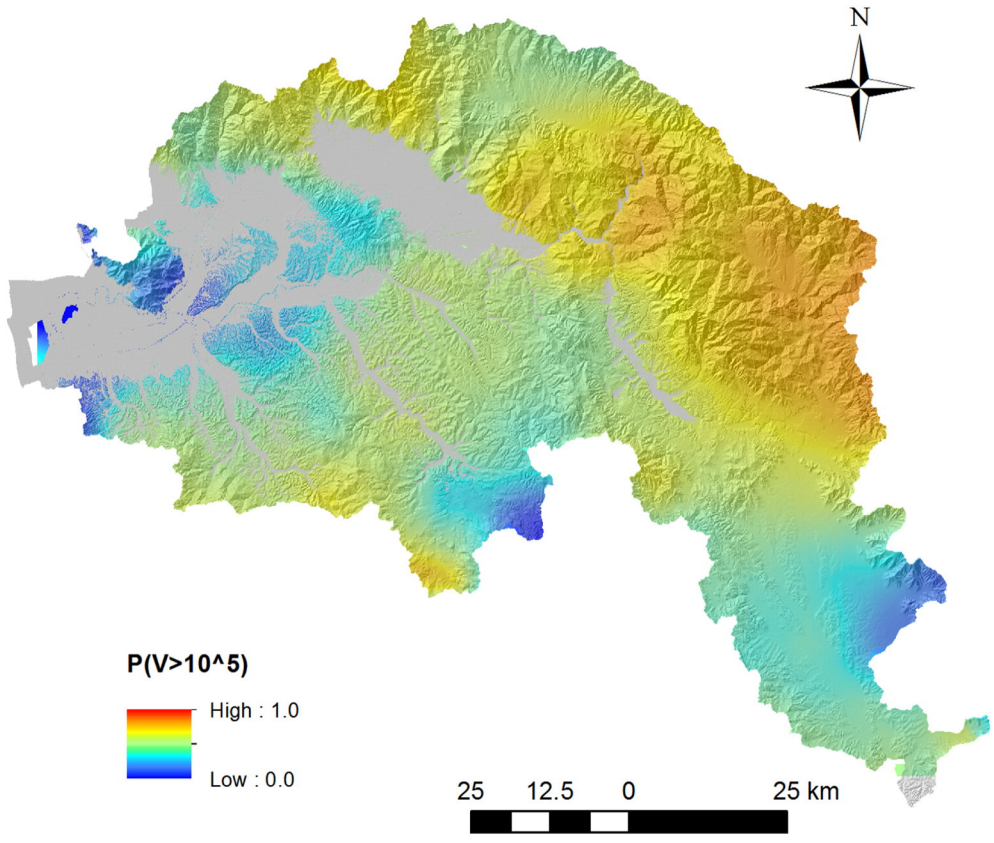

Fig. 11. Exceedance probability map relative to a landslide volume $V > 10^5$ m^3. This type of map may have a notable importance in landslide risk assessment at the basin scale when modelling landslide intensity in terms of magnitude and volume.

5. Conclusions

We have developed a simple approach for describing the spatial pattern of volume frequency distribution for landslides. This kind of support may be used for mapping landslide magnitude at different scales to study the causal relationships between mass wasting and environmental factors. The application to the Arno river basin in Central Italy shows that a strong correlation exists between mobilized volumes and valley width at the 10 km scale, whilst at larger scales tectonic forcing and lithology play a more important role, mainly because they condition the dynamic equilibrium of rock uplift and erosion rates and the balance of cohesive versus frictional forces in the hillslope materials. Further research is needed to explore other aspects of the spatial distribution of MFDs of landslides and natural hazards in general, such as the definition of a simple expression for the left part of the distribution. The use of a second spatial parameter, representing smaller mass movements, would be of notable interest for increasing the range of landslide volumes which can be considered within the prediction mapping.

Acknowledgments

The original version of the data set used in this research was made available by the Arno River Basin Authority, to which we are grateful. We also thank the editor Takashi Oguchi and the referees Ian S. Evans and Lucien D. Dragut for their careful revision of the manuscript and suggestions and comments which contributed to improve the paper. The landslide inventory used is available upon request.

Appendix A. Supplementary data

Supplementary data associated with this article can be found in the online version, at http://dx.doi.org/10.1016/j.geomorph.2016.08.032. These data include the Google map of the most important areas described in this article.

References

Bak, P., Tang, C., Wiesenfeld, K., 1988. Self-organized criticality. Phys. Rev. A 38, 364.
Balestrieri, M.L., Bernet, M., Brandon, M.T., Picotti, V., Reiners, P., Zattin, M., 2003. Pliocene and Pleistocene exhumation and uplift of two key areas of the Northern Apennines. Quat. Int. 101–102, 67–73.
Bianchi, F., Catani, F., 2002. Landscape risk management in Northern Apennines (Italy). Environmental Studies, Ninth International Conference on the Modelling, Monitoring and Management of Environmental Problems 7. ENVIROSOFT 2002, Bergen, Norway, pp. 319–328 6–8 May 2002.
Bicocchi, G., Vannocci, P., Nocentini, M., Tacconi-Stefanelli, C., Masi, E.B., Carnicelli, S., Tofani, V., Catani, F., 2015. Preliminary assessment of the factors controlling the geotechnical and hydrological properties in the hillslope deposits of eastern Tuscany (Central Italy). Proceeding of 17th Annual Conference of the International Association for Mathematical Geosciences, Freiberg (Saxony) Germany, pp. 865–874.
Bicocchi, G., D'Ambrosio, M., Rossi, G., Rosi, A., Tacconi-Stefanelli, C., Segoni, S., Nocentini, M., Vannocci, P., Tofani, V., Casagli, N., Catani, F., 2016. Shear strength and permeability in situ measures to improve landslide forecasting models: a case study in the Eastern Tuscany (Central Italy). Proceeding 12th ISL 2016 Congress, Napoli, Italy.
Boccaletti, M., Bonini, M., Moratti, G., Sani, F., 1995. Nuove ipotesi sulla genesi e l'evoluzione dei bacini post-nappe in relazione alle fasi compressive neogenico-quaternarie dell'Appennino Settentrionale. Scritti e Documenti dell'Accademia Nazionale delle Scienze. 14, pp. 229–262 In Italian.
Brardinoni, F., Church, M., 2004. Representing the landslide magnitude-frequency relation: Capilano River basin, British Columbia. Earth Surf. Process. Landf. 29 (1), 115–124.
Bras, R.L., Rodriguez-Iturbe, I., 1985. Random Functions and Hydrology. Addison-Wesley, Reading, MA.
Brunetti, M.T., Guzzetti, F., Rossi, M., 2009. Probability distributions of landslide volumes. Nonlinear Process. Geophys. 16, 179–188.
Brunsdon, C., Fotheringham, A.S., Charlton, M.E., 1996. Geographically weighted regression: a method for exploring spatial nonstationarity. Geogr. Anal. 28 (4), 281–298.
Canuti, P., Casagli, N., Catani, F., Fanti, R., 2000. Hydrogeological hazard and risk in archaeological sites: some case studies in Italy. J. Cult. Herit. 1 (2), 117–125.
Carrara, A., Cardinali, M., Detti, R., Guzzetti, F., Pasqui, V., Reichenbach, P., 1991. GIS techniques and statistical models in evaluating landslide hazard. Earth Surf. Process. Landf. 16, 427–445.
Casagli, N., Catani, F., Puglisi, C., Delmonaco, G., Ermini, L., Margottini, C., 2004. An inventory-based approach to landslide susceptibility assessment and its application to the Virginio river basin, Italy. Environ. Eng. Geosci. 10 (3), 203–216.
Catani, F., Casagli, N., Ermini, L., Righini, G., Menduni, G., 2005. Landslide hazard and risk mapping at catchment scale in the Arno River basin. Landslides 2 (4), 329–342.
Catani, F., Segoni, S., Falorni, G., 2010. An empirical geomorphology based approach to the spatial prediction of soil thickness at catchment scale. Water Resour. Res. 46 (5), W05508.
Catani, F., Lagomarsino, D., Segoni, S., Tofani, V., 2013. Landslide susceptibility estimation by random forests technique: sensitivity and scaling issues. Nat. Hazards Earth Syst. Sci. 13, 2815–2831.
Clauset, A., Shalizi, C.,.R., 2009. Power-law distributions in empirical data. SIAM Rev. 51 (4), 661–703.
Convertino, F., Troccoli, A., Catani, F., 2013. Detecting fingerprints of landslide drivers: a MaxEnt model. J. Geophys. Res. 118, 1367–1386.
Corominas, J., van Westen, C.J., Frattini, P., Cascini, L., Malet, J.P., Fotopoulou, S., Catani, F., Van den Eeckhaut, M., Mavrouli, O., Agliardi, F., Pitilakis, K., Winter, M.G., Pastor, M., Ferlisi, S., Tofani, V., Hervas, J., Smith, J.T., 2013. Recommendations for the quantitative analysis of landslide risk. Bull. Eng. Geol. Environ. 73, 209–263.
Cruden, D.M., Varnes, D.J., 1996. Landslide types and processes. In: Turner, A.K., Schuster, R.L. (Eds.), Landslides Investigation and Mitigation. National Research Council, Transportation Research Board, Washington, DC, pp. 36–75.
Cyr, A.J., Granger, D.E., 2008. Dynamic equilibrium among erosion, river incision, and coastal uplift in the northern and central Apennines, Italy. Geology 36 (2), 103–106.
Dai, F.C., Lee, C.F., 2001. Frequency volume relation and prediction of rainfall-induced landslides. Eng. Geol. 59, 253–266.
D'Anastasio, E., De Martini, P.M., Selvaggi, G., Pantosti, D., Marchioni, A., Maseroli, R., 2006. Short-term vertical velocity field in the Apennines (Italy) revealed by geodetic levelling data. Tectonophysics 418 (3), 219–234.
Fan, X., van Westen, C.J., Xu, Q., Gorum, T., Dai, F., 2012. Analysis of landslide dams induced by the 2008 Wenchuan earthquake. J. Asian Earth Sci. 57, 25–37.
Fell, R., Corominas, J., Bonnard, C., Cascini, L., Leroi, E., Savage, W.Z., 2008. Guidelines for landslide susceptibility, hazard and risk zoning for land-use planning. Eng. Geol. 102 (3–4), 99–101.
Frattini, P., Crosta, G.B., 2013. The role of material properties and landscape morphology on landslide size distributions. Earth Planet. Sci. Lett. 361, 310–319.
Guthrie, R.H., Evans, S.G., 2004. Analysis of landslide frequencies and characteristics in a natural system, coastal British Columbia. Earth Surf. Process. Landf. 29, 1321–1339.
Guzzetti, F., Malamud, B.D., Turcotte, D.L., Reichenbach, P., 2002. Power-law correlations of landslide areas in central Italy. Earth Planet. Sci. Lett. 195, 169–183.
Guzzetti, F., Ardizzone, F., Cardinali, M., Rossi., M., Valigi, D., 2009. Landslide volumes and landslide mobilization rates in Umbria, central Italy. Earth Planet. Sci. Lett. 279 (3–4), 222–229.
Hungr, O., 1997. Some methods of landslide hazard intensity mapping. Landslide risk assessment. Landslide Risk Assessment. Balkema, Rotterdam, pp. 215–226.
Larsen, M.C., Torres-Sanchez, A.J., 1998. The frequency and distribution of recent landslides in three montane tropical regions of Puerto Rico. Geomorphology 24, 309–331.
Malamud, B.D., Turcotte, D.L., 1999. Self-organized criticality applied to natural hazards. Nat. Hazards 20, 93–116.
Malamud, B.D., Turcotte, D.L., 2006. The applicability of power-law frequency statistics to floods. J. Hydrol. 322 (1–4), 168–180.
Malamud, B.D., Turcotte, D.L., Guzzetti, F., Reichenbach, P., 2004. Landslide inventories and their statistical properties. Earth Surf. Process. Landf. 29, 687–711.
Martini, I.P., Vai, G.B., 2001. Anatomy of an Orogen: the Apennines and Adjacent Mediterranean Basins. Kluwer Acad. Publ., Dordrecht 632 pp.
Press, W.H., Teukolsky, S.A., Vetterling, W.T., Flannery, B.P., 1992. Numerical Recipes in C: the Art of Scientific Computing. 2nd ed. Cambridge University Press, Cambridge, UK.
Rodriguez-Iturbe, I., Rinaldo, A., 1997. Fractal River Basins: Chanca and Self-Organization. Cambridge University Press, Cambridge, UK.
Roering, J.J., Mackey, B.H., Handwerger, A.L., Booth, A.M., Schmidt, D.A., Bennett, G.L., Cerovski-Darriau, C., 2015. Beyond the angle of repose: a review and synthesis of landslide processes in response to rapid uplift, Eel River, Northern California. Geomorphology 236, 109–131.
Soeters, R.C., Van Westen, J., 1996. Slope instability recognition, analysis and zonation. In: Turner, A.K., Schuster, R.L. (Eds.), Landslides, Investigation and MitigationTransportation Research Board, National Research Council, Special Report 247. National Academy Press, Washington, USA, pp. 129–177.
Stark, C.P., Guzzetti, F., 2009. Landslide rupture and the probability distribution of mobilized debris volumes. J. Geophys. Res. 114, F00A02.
Stark, C.P., Hovius, N., 2001. The characterization of landslide size distribution. Geophys. Res. Lett. 28, 1091–1094.
Tacconi-Stefanelli, C., Segoni, S., Casagli, N., Catani, F., 2016. Geomorphic indexing of landslide dams evolution. Eng. Geol. 208, 1–10.
Trigila, A., Iadanza, C., Spizzichino, D., 2010. Quality assessment of the Italian landslide inventory using GIS processing. Landslides 7 (4), 455–470.
Tucker, G.E., Catani, F., Rinaldo, A., Bras, R.L., 2001. Statistical analysis of drainage density from digital terrain data. Geomorphology 36 (3), 187–202.
Turcotte, D.L., Malamud, B.D., 2004. Landslides, forest fire and earthquake: examples of self-organized critical behaviour. Physica A 340 (4), 580–589.
Van Den Eeckhaut, M., Poesen, J., Govers, G., Verstraeten, G., Demoulin, A., 2007. Characteristics of the size distribution of recent and historical landslides in a populated hilly region. Earth Planet. Sci. Lett. 256, 588–603.